Assessing Seismic Vulnerability and Site Response in Varanasi City, India

Singh Manjari[1*], Duggal Shashi Kant[2] and Singh V.P.[2]
1. Structural Engineering Department, VJTI Mumbai, INDIA
2. Civil Engineering Department, MNNIT Allahabad, Prayagraj, U.P., 211004, INDIA
*manjarisingh.2508@gmail.com

Abstract
Proximity of the highly stressed Faizabad ridge to Varanasi City and the unavailability of earthquake ground motion records necessitates a stochastic approach to study the deterministic seismic scenario of Varanasi city. The current study consists of 1D site response analysis of Varanasi city along Indus-Ganga plain. Details of boreholes for 30 sites across the city are used in the analysis. Synthesis of strong ground motions has been done for Azamgarh fault using stochastic finite fault model. The site response analysis results have been represented as surface acceleration time history (TH), response spectra and PGA contour. Estimated average response spectra at surface level are compared with IS-1893:2016 code which reveal that spectral acceleration values are presently underestimated at many places in Varanasi which would be a great risk from potential earthquakes in near future.

Keywords: Varanasi City, Stress Drop, Deep Soil, Site Amplification and Response Spectra.

Introduction

Earthquakes are among the most hazardous and destructive events, causing significant human losses and structural damage. Their unpredictability can lead to multiple hazards including site impact, liquefaction, ground displacement, explosions, landslides and tsunamis. Factors such as high population density, insufficient planning and substandard construction practices have increased seismic risk. Several major earthquakes have originated from subduction zones including the 1905 Kangra, 1934 Bihar-Nepal, 1960 Great Chile, 1985 Mexico, 1989 Loma Prieta, 2004 Sumatra and 2011 Sendai earthquakes. Subduction areas with seismic strain gaps exacerbate the situation by generating large-scale earthquakes.

The recurrence of low-intensity earthquakes in the Himalayan region should not be dismissed; instead, these events must be viewed as indicators of a potentially massive earthquake in the near future, particularly in the central Himalaya seismic strain gap. Despite many advances in earthquake-resistant structural design, a more thorough understanding and improved construction practices are still necessary to reduce loss of life and severe structural damage. Due to explosive population growth and the seismicity of the area, cities neighboring the highly seismic Himalayan zone urgently require seismic microzonation. India has experienced numerous powerful earthquakes over the centuries, with approximately sixty percent of the nation vulnerable to seismic hazard damage[25]. Determination of hazard parameters (PGA and response spectrum) is necessary for design of buildings which is helpful in seismic hazard planning and management. This research is crucial and should be conducted in cities near or within highly active seismic areas, like those in India where major earthquakes occur relatively frequently, for example in active areas in India. Assessment of earthquake hazard at micro level is a major step in microzonation study where impacts are computed and mapped.

Previously many researchers have presented earthquake hazard maps of Indian cities such as Bangalore City[1], Imphal[31], Kolkat[14], Gujarat[35], Kanpur[17], Haryana[28], Mumbai City[10], Vijayawada city[34], Surat[37], Chennai city[23] and Vishakhapatnam[29] etc. These studies primarily focus on region-specific responses based on local soil properties and "N" values of subsurface layers. Important parameters for performing site response analysis include soil thickness, type, density, plasticity index, groundwater table and shear wave (SW) velocity, which can be derived from the relationship between SW velocity and "N" values.

Although site response studies have been conducted by many authors in different cities but there is no literature available for Varanasi city, which is an old living city, clustered with ancient heritage structures, temples and archaic buildings. The city is located in the IGP and is prone to earthquakes as it is in the vicinity of the Himalayas. In addition, the high population density of the city increases its vulnerability to disasters. Considering these factors, it is necessary to conduct a site response analysis for Varanasi City.

In this research work, Varanasi city has been selected for earthquake hazard assessment due to its historical and industrial importance. All seismic activities and sources within 450-km radius of Varanasi city are considered. A contour map is prepared for representation of results of 5% damped response spectrum and spectral acceleration. This will help the design engineers and construction agencies to assess the seismic response of the sites and also to select a suitable site for important projects.

About the City Varanasi and Geology

The city Varanasi is situated on the bank of the Ganga (Ganges) river. Two other small rivers Varuna and Assi flow

in the north and south of the city respectively[38]. Varanasi city lies between the parallels of 25^0 15'0" to 25^0 20'22" N and 82^0 56'44" to 83^0 4'10" E and central coordinates are 25^0 19'18.06"N-82^0 59'14.24"E and located in east of Uttar Pradesh State (Fig. 1). This region is situated about 50 kilometers north of the Vindhyan range, which borders the Ganga basin in the south and forms the northern peripheral cratonic bulge.

Geological Characteristics of Varanasi District

Varanasi region is underlained by alluvium sediments of quaternary age. On the basis of lithological character Varanasi region is categorized as Older and Newer Alluvium[36]. Gangetic older alluvium plain belongs to the middle to late Pleistocene age and lies above the highest floodplain limits of rivers. Newer alluvium plain belongs to present era and lies within the floodplain limits. The newer alluvium is made up of fine to medium grained sand, silt and small fraction of clay. The older alluvium is dark in color having clay, kankar (harder and coarser material of various shape and size) and is rich in lime content[13]. The Varanasi older alluvial plain describes the ancient geomorphological surface in the plains of Ganga which occurs at the greatest tectonic stage. Ganga is flowing in the south of the Varanasi region, forming a crescent shape which causes deposition of coarser sediments on its western bank between Rajghat (North) and Samneghat (South) due to the fluvial process.

Material and Methods

In the present study, 110 borehole data are gathered from different organizations for Varanasi city and analyzed for their response by subjecting to input motions. The data are well scattered along the city. The location of boreholes is shown in fig. 1. The collected borehole data at these sites include necessary information such as "*N*" value, depth, water content and index property of soil. "*N"* values refer standard penetration *N* value i.e. SPT (N) which is obtained by the standard penetration test. It gives information about soil strength.

"*N*" values have been used for the calculation of SW velocity from the relation (1) proposed by Singh et al[38] for Varanasi city:

$$V_s = 70.05\, N^{.49} \quad (1)$$

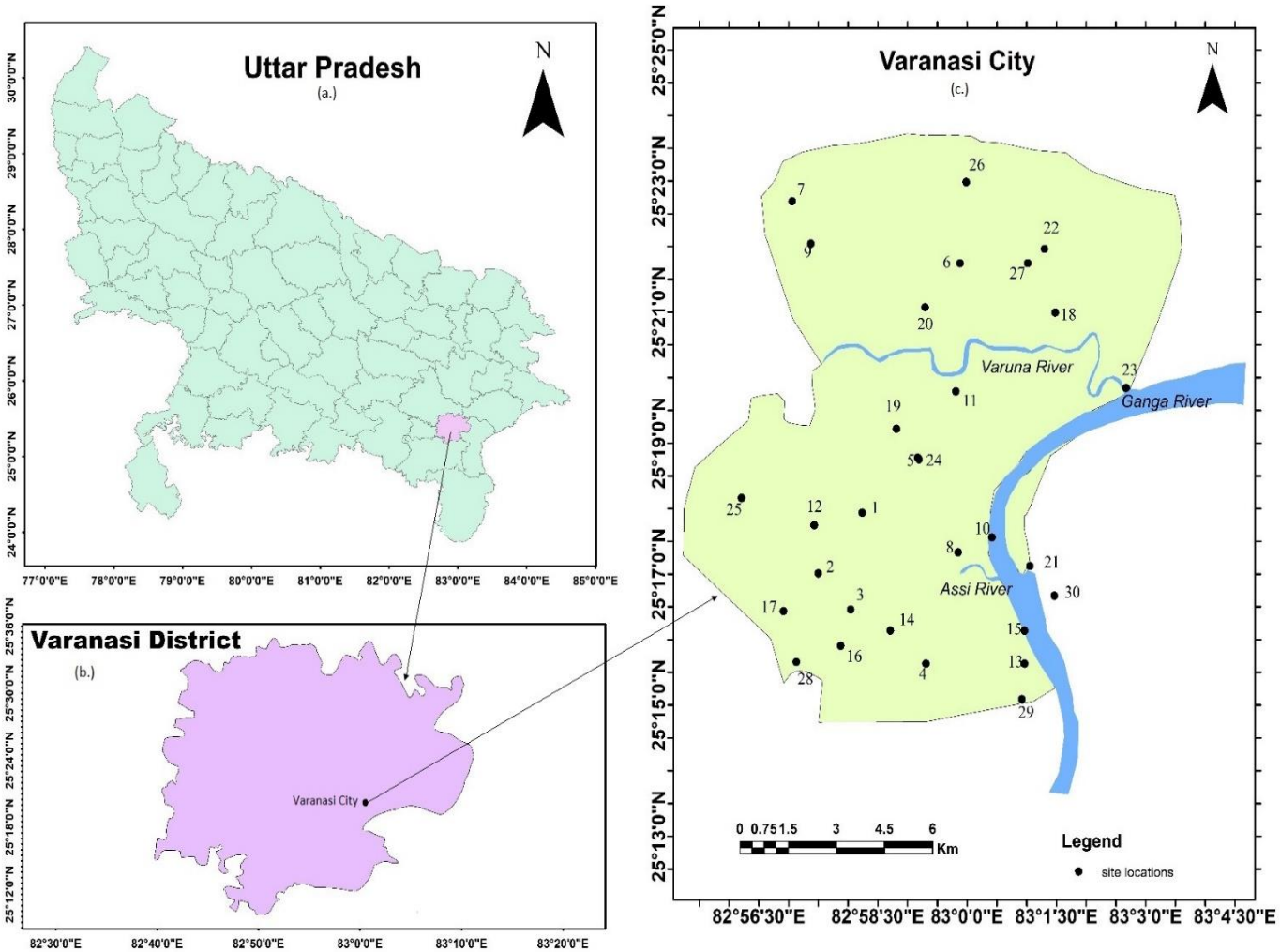

Fig. 1: (a) Location of Varanasi District in State Map. (b) Location of Varanasi city in District Map and (c) Site locations in city map

SW at 30 m depth is important for the classification of soil. According to classification proposed by IBC 2009[15] based on V_{s30} value, it is determined as:

$$V_{s30} = \frac{\sum_{i=1}^{n} d_i}{\sum_{i=1}^{n} \frac{d_i}{V_{si}}} \quad (2)$$

where n is the number of layers in the top 30 m, d_i and V_{si} are the thickness $[m]$ and the SW is velocity [m/s] of the i^{th} layer respectively. Most of the sites fall in category *C* and *D* type[15]. SW velocity profile for site Ramna and Awaleshpur is presented in figure 2.

Regional Seismicity and Seismotectonics: IGP and is geologically a foredeep basin of the Himalayan foreland, is made up by extension of basement rocks and depression. This plain is having thick alluvial deposits which make this foreland vulnerable to seismic threat. The Indian Standards code (IS 1893:2016)[16] has classified the entire IGP area in seismic Zones $II - V$ with a PGA (0.1-0.36 g). The lowest hazard zone designated as II is the southwest portion of the IGP, whereas central part of the IGP is marked as zone III which covers most of the cities (Varanasi, Lucknow, Kanpur etc.). The Gangetic plain has corrugated inequalities and buried ridges such as Delhi-Haridwar Ridge which stretches from New Delhi – Garhwal, trending NNE-SSW, Delhi-Muzaffarnagar ridge runs along New Delhi to Kathgodam (Nepal), trends east to west. Faizabad ridge runs from Allahabad to Kanpur in E-W direction and progresses to N-E direction towards Lucknow and continues to Himalaya (Nepal)[18].

Faizabad ridge, near to the city, is quiescent over more than 300 years mentioned by Disaster Risk Management Programme organized by the Home Affairs Ministry in collaboration with UN Development Programme (UNDP). Due to vast seismic gap, ridge is substantially stressed and has the capacity to produce higher magnitude of earthquake in upcoming years[39]. Many identified faults (Great Boundary, Azamgarh, Lucknow fault, East and West Patna Fault and Munger-Saharsa) are presented in Indian Seismo-tectonic map[11]. The Faizabad and Munger ridge, near to Varanasi, is surrounded by many faults which are the extension of Bundelkhand and Satpura massif. The IGP is comparatively moderately seismic from the Himalayas[30].

Varanasi, one of the heritage city of India belongs to zone III[16]. The city has customarily faced tremors in the past when higher intensity quakes struck the neighboring vicinities of the Himalayan territory. Some notably calamitous earthquakes that occurred in Uttar Pradesh and neighboring country and felt by the city are: M_w 6.2, 1956 Bulandshahar earthquake, M_w 5.7, 1965 Gorakhpur earthquake and M_w 5.8, 1966 Moradabad earthquake, Countrywide M_w 7.5, 1916 Dharchulla earthquake, M_w 6.5, 1945 Uttarakhand earthquake, M_w 6.8, 1991 Uttarkashi earthquake, M_w 6.0, 1997 Jabalpur earthquake, M_w 6.8, 1988 Bhar- Nepal earthquake, M_w 8.4, 1934 Nepal-Bihar earthquake and M_w 7.8, 2015 Nepal earthquake.

Approximately 500 mortalities were recorded in 1833 Nepal Earthqauke (M_w 7.6). MM intensity VI-VII was felt in Varanasi during 1934 Bihar-Nepal earthquake (Mw 8.1). 1988 Bihar-Nepal earthquake (Mw 6.8) occurred in eastern Nepal and India causing widespread damage. The Mw 7.8 earthquake in Nepal in 2015 was deadliest catastrophe ever. It claimed over 9,000 deaths, wounded countless people, over 50,000 homeless people and the total economic loss exceeded the country's GDP levels. Seismic Intensity of IV–VII was also recorded in IGP and range between IV–V intensity was felt in Varanasi region[11,24,26].

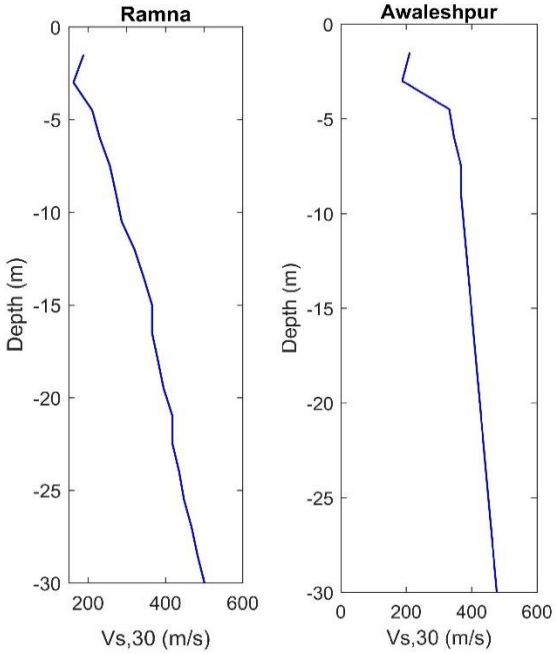

Fig. 2: Shear Wave Velocity Profile for site Ramna and Awaleshpur

In the present study, faults around Varanasi are plotted between latitude 25.28º N – 29.28º N and longitude 78.96º E – 86.96º E (around 450 km) using MATLAB and are shown in fig. 3.

Among the various fault around the city as shown in fig. 2., Azamgarh fault is near to the city and gives maximum value of PGA during simulation. Therefore, Azamgarh fault is further taken for simulating ground motions. Fault details were taken from literature like Dasgupta et al[11] and Kayal[18] shown in table 1.

Ground Motion Simulation: Strong ground motion records for Varanasi are not available in the literature. In the regions where historical database of strong ground motions is unattainable, modified records may be achieved by generating synthetic records. In this study, stochastic finite-fault model[4,5] was used to simulate strong ground motion record. Further simulated ground motions are helpful in deriving response spectra. According to the model, rectangular fault plane is disintegrated into small subfaults. Each subfault signifies a point source described by ω^2 spectrum[7,8]. Ruptures begin at hypocenter and progress kinematically until each subfault triggers. Acceleration Fourier amplitude spectrum of the j^{th} subfault at R_j distance, stated as source, path and site effects, can be estimated as eq. (3):

$$A_j(f) = \left(\frac{M_j H_j (2\pi f)^2}{1+\left(f/f_{0j}(t)\right)^2}\right)\left(\frac{\sqrt{2}\langle R_{\theta\emptyset}\rangle}{4\pi\rho V_s^3}\right)\left(Ge^{\frac{\pi f R_j}{V_s Q}}\right)\left(F(f)e^{-\pi f k_0}\right) \quad (3)$$

In eq. (3), R_j is the subfault distance from the site, V_s is the shear-wave velocity, f corresponds to frequency, $R_{\theta\emptyset}$ indicates radiation pattern, $F(f)$ denotes amplification due to free surface where the shear-wave velocity is about 3.6 km/sec toward the surface, where the average SW velocity may be less than 1500 m/sec.

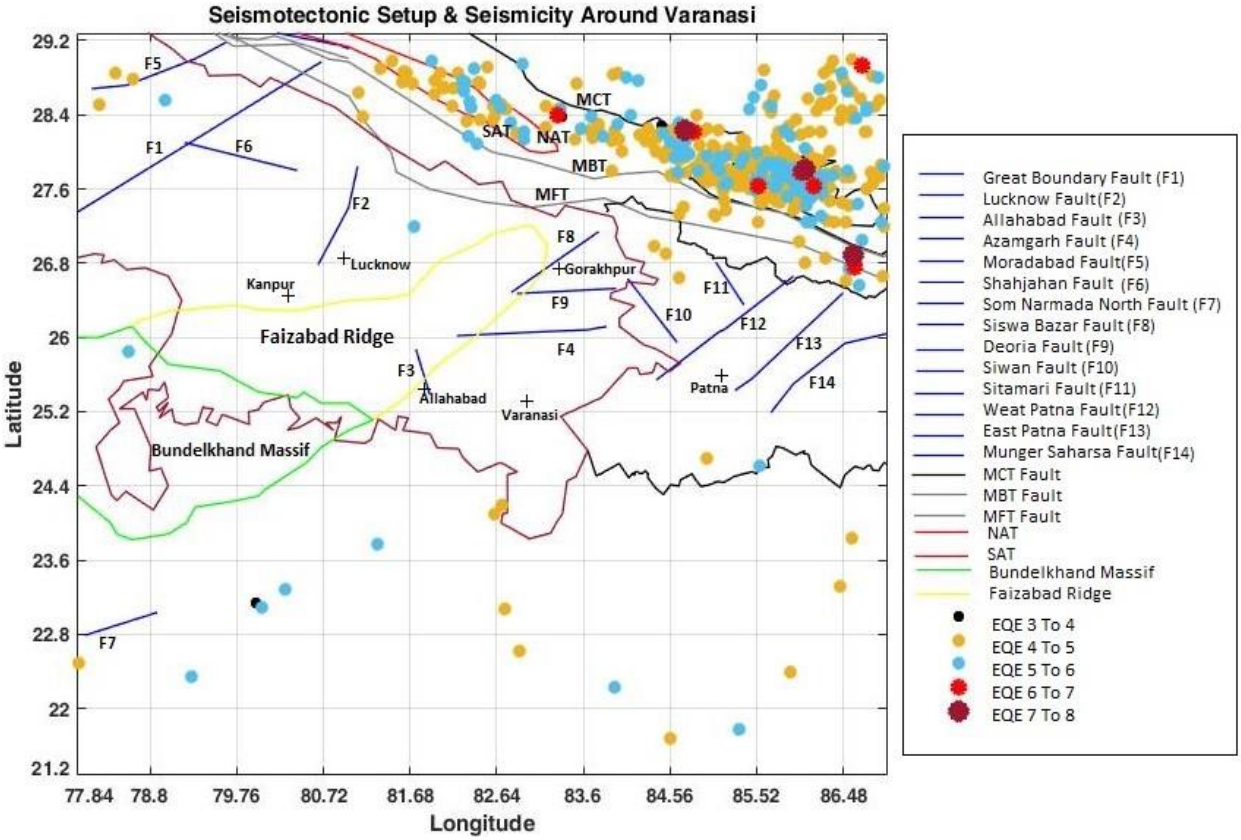

Fig. 3: Seismicity around the city[38]

Table 1
Propperties of Azamgarh Fault

Length (km)	**158**
Position	Subsurface
Strike (Deg.)	87
Dip (Deg.)	50
Latitude	26, 26.074
Longitude	82.19 83.778
M_{max} (as per WC 1994)	6.9

where ρ is density of the crust at the focal depth, f_{0j} is the corner frequency, Q is frequency-dependent quality factor, G denotes geometrical spreading term, k_0 is Kappa telling about the decay of acceleration at high frequency[2]. The coefficient $\sqrt{2}$ in the above equation arises as the product of the free surface amplification and partitioning of energy in orthogonal directions and scaling factor (H_j). Eq. 7 which is used in conserving radiated energies at higher frequency and balancing spectrum range of the subfaults also[22]:

The moment of the j[th] subfault M_j is determined from slip distribution i.e. ratio of its area to the area of the main fault and is defined in eq. 4:

$$\mathrm{M_j} = \frac{\mathrm{M_0 D_j}}{\sum_{j=1}^{T} \mathrm{D_j}} \tag{4}$$

where $\mathrm{D_j}$ is average final slip acting on the jth sub fault, $\mathrm{M_0}$ is seismic moment of all sub faults, defined as ($\mathrm{M_0} = \mu \overline{u} A$) where μ is the shear modulus or rigidity which is assumed to be constant at the crustal level, $\overline{u}$ is average slip and A is fault area.

The conventional finite fault method has some drawbacks which include limiting the number of active subfaults and dependence of radiated energy on subfault size. Motazedian and Atkinson[22] have implemented a dynamic corner frequency concept in which corner frequencies were considered as dynamic parameters that decrease over time as the rupture becomes larger. The dynamic corner frequency (f_{0j}), of the jth subfault, with $N_R(t)$ as cumulative number of ruptured sub faults at (t)time and $\Delta\sigma$ as stress drop, is expressed in eq. 5:

$$f_{0j}(t) = 4.9 \times 10^6 \left(N_R(t)\right)^{-(1/3)} N^{-1/3} V_s \left(\frac{\Delta\sigma}{M_0}\right)^{(1/3)} \tag{5}$$

The scaling factor, H_j for jth sub-fault can be obtained using the following relation (Eq. 6):

$$H_j = \left(N \frac{\sum_f \left(\frac{f^2}{1+(f/f_0)^2}\right)^2}{\sum_f \left(\frac{f^2}{1+\left(f/f_{0j}(t)\right)^2}\right)^2} \right)^{(1/2)} \tag{6}$$

where f_0 denotes the corner frequency of the rupture, estimated by taking $N_R(t) = N$ as in eq. 5.

In the present study, finite-fault seismological model has been enforced in the time domain by using numerical simulation for which Boore[7] suggested the following three steps:

1) Simulated strong motion duration would be considered equal to the Gaussian stationary white noise sample of length[3].

$$T = 1/f_c + 0.05r \tag{7}$$

2) To bring in the non-stationarity in the ground motion, this sample is multiplied by the modulating function of Rodolfo and Hart. After which Fourier spectrum completely changes into the frequency domain from time domain. By using root mean squares value, Fourier spectrum is normalized and the normalized values are multiplied to the terms as in eq. 3.

3) To acquire a sample of sub-surface acceleration time history, the derived function is converted back again to time domain. To estimate ground motion acceleration $A(t)$ because of entire fault, the acceleration time histories are added up with the time delay Δt_i expressed as:

$$A(t) = \sum_{i=1}^{K} A_i(t + \Delta t_i) \tag{8}$$

It has been reported that if initial source and medium parameters are familiar one, then inferring the ground motion by using Stochastic finite fault simulation would become more computive. Recently this finite fault seismological model has been applied for NE India[32] and for Imphal city[27,31]. Modification between bedrock and A-type sites is a linear problem which is in one dimensional and therefore these sites augmentation can be encountered by using directly the quarter wavelength method of Boore et al[6]. Chandler et al[9] assembled the database of Kappa factors for different parts of the world. To determine the kappa factors from the average SW velocity in top 30 m of soil, they have given empirical equation as:

$$k_0 = \frac{0.057}{V_{s30}^{0.8}} - 0.02 \tag{9}$$

For simulating rock level ground motion at Varanasi, the kappa factor for soft rock site is obtained as 0.057 using eq. 9. In the present study, table 2 shows the parameters used to simulate the synthetic ground motion. Based on the above proposed theory ground motions are synthesized using EXSIM software, which is based on stoachastic finite-fault method. On the basis of seismicity of region, Azamgarh fault was selected for simulation.

Moment magnitude M_w is estimated by Wells and Coppersmith[42] relation (Eq. 10) using fault rupture length as $1/3\, rd$ of total fault length[19].

$$M_w = 4.38 + 1.49 * \log(RLD) \text{ (All rupture types)} \tag{10}$$

where M_w= moment magnitude; SRL= surface rupture length (km); RLD= sub-surface rupture length (km).

Estimation of design M_w value of a region involves considerable amount of uncertainty to estimate maximum magnitude of earthquake in a region depending on geological evidence, tectonic evidence and historical seismicity.

Table 2
Parameters considered for simulation.

Parameters	**Details**
Earthquake MagnitudeM_w (WC 1994)	6.9
Fault length, Strike, Dip (Degree)	158 km, 87 °, 50 °
Depth of fault	3.5 km
Source to Site Distance	*111 km*
Density at source	2.9 g/cc
V_s	3500 m/s[20,40]
$\Delta\sigma$	200 bars[18]
$Q(f)$	$142f^{1.04}$ [21]
G Geometric attenuation	$^1/_r$ $(for\ r \leq 100\ km)$;$\sqrt{1\ /\ (100r)}$ $(for\ r > 100\ km)$[40]
k_o	0.057 for deep profiles
$\Delta\sigma$ Reference stress drop	100 bars
Pulsing percentage and Sub fault size	50% and 0.25 km × 0.25 km
Crustal amplification	ENA Hard rock amplification[3]

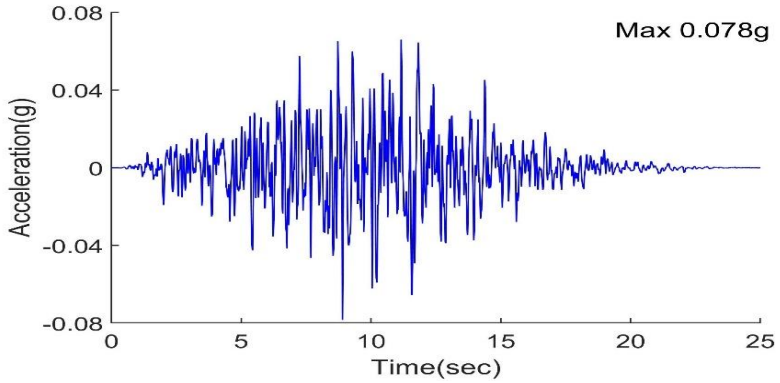

Fig. 4: Simulated acceleration time History

Using the above parameters, effective simulation for Azamgarh fault was carried out, which gives *bedrock Acceleration TH* with max PGA of 0.078 g for the city (Fig. 4). The synthesized time histories are used further as input for site analysis of Varanasi city.

Methodology: Site response study involves the analysis of response of soil deposits during the application of time histories to the layers of soil profile. This analysis is used to obtain ground surface motion in order to evaluate amplification potential and to develop response spectras. The basis of a 1-D site response analysis includes propagation of S-waves in vertical direction across soil layer resting on elastic rock layer that stretches to infinite depth.

Generally, linear, equivalent linear and non-linear approaches are used to carry out site response analysis. The main difference between linear and equivalent linear approach is in estimation of shear modulus value. All other formulations are same except initial modulus (in case of linear analysis) whereas the secant modulus is used in the equivalent linear analysis. Theoretically, in equivalent linear analysis, it is considered that angle of incidence of propagating wave from bedrock to above soil layer is perpendicular to the interface due to the effect of Snell's law. G, ξ and ρ are shear modulus, damping ratio and density of the soil layers respectively.

In this research, 1-D equivalent linear site response analysis has been performed using DeepSoil software for all sites of the Varanasi city. The hyperbolic model is selected and optimized using data from the EPRI[12] curves for 300-m-thick soil column. V_s profiles for Varanasi city for 30 sites have been computed using eq. 1. It is assumed that surficial top layer is underlain by rock so modification of acceleration time history, which is one dimensional nonlinear problem (i.e. reduction of shear modulus and increase of damping ratio with increasing/ decreasing shear strain) between rock and soil site, is required.

Curves between damping ratio versus shear strain and shear modulus versus shear strain given by Vucetic and Dobry[41] for clay and sand based on plasticity properties have been used to account for the nonlinear characteristics of soil. Generated synthetic bed rock ground motion is input for site specific response analysis. The analysis results are shown in the form of surface acceleration TH, response spectrum for 5% damping.

Results and Discussion

A detailed series of analysis were performed to obtain the ground motion and response spectra of all the 30 sites at surface level. The simulated TH was applied at bedrock level as input to estimate the responses of the sites. Simulations for ground motion time histories were done for Azamgarh fault for stress drop 200 bar with 0.06 of Kappa value applied at the level of 300-meter-thick soil column (below the depth of 30 meter).

Acceleration time data (Input/output ground motions and average acceleration) of all 30 places were compiled and plotted for Varanasi as depicted in fig. 5. Contour lines for PGA values corresponding to synthesized ground motion with 200 bar stress drop are plotted to obtain a clear view of ground motion variation throughout the city (Fig. 6). Further generated response spectra were compared to regular Indian response spectra (IS 1893:2016) (Fig. 7). Figure 5 shows the plot of surface TH obtained from the analysis. Estimated maximum output PGA at surface was 0.20 g when input acceleration of 0.078 g was applied at the rock level. This specifies that ground acceleration at the bedrock level amplified by 2.5 times on the ground level. Minimum estimated PGA value was found to be 0.06 g. Surface acceleration values for all 30 sites are listed in table 3.

A surface level PGA contour plot has been shown in fig. 6). It can be noticed that Awaleshpur which lies in the southern part of the city shows maximum PGA output value whereas Samneghat shows minimum PGA value, this site has proximity to Ganga River with shallow bedrock depth. Awaleshpur, Ahileshpur, Sarnath and Parmanandpur are some sites where amplification is much higher than the other sites of Varanasi. We can also infer from the figure that southern portion of Varanasi has higher PGA which can cause more damages to structures.

Table 3
Estimated PGA values for different sites

S.N.	Site Name	Latitude	Longitude	PGA (g)
1	Manduwadih	25.2989	82.9706	0.10
2	DLW Ground	25.2835	82.9583	0.09
3	Newada	25.2743	82.9674	0.13
4	BHU	25.2605	82.9884	0.13
5	Nagar Nigam	25.3129	82.9861	0.09
6	Daulatpur	25.3623	82.9980	0.13
7	Lodhan	25.3781	82.9510	0.17
8	Bhelupur	25.2888	82.9975	0.12
9	Parmanandpur	25.3673	82.9562	0.14
10	Imliya Ghat	25.2926	83.0069	0.12
11	Chauka Ghat	25.3297	82.9968	0.11
12	Kanchanvihar Colony Maduwadih	25.2957	82.9571	0.10
13	Laharthara	25.2605	83.0160	0.14
14	Mahamanapuri	25.2689	82.9784	0.12
15	SamneGhat	25.2689	83.0160	0.08
16	Awaleshpur	25.2650	82.9646	0.20
17	Pahadi	25.2739	82.9485	0.12
18	Panchkoshi Shivpur	25.3498	83.0246	0.10
19	Pandeypur	25.3203	82.9802	0.10
20	Policeline	25.3512	82.9882	0.11
21	Katesar	25.2854	83.0175	0.13
22	ROB Sarnath	25.3660	83.0216	0.14
23	Sarai Muhana	25.3306	83.0445	0.13
24	Sigra	25.3125	82.9865	0.12
25	Lohta	25.3026	82.9368	0.13
26	Goithara Sarnath	25.3830	82.9997	0.14
27	Income Tax Colony Sarnath	25.3624	83.0170	0.09
28	Amara,Akhileshpur	25.2539	82.9529	0.19
29	Ramna	25.2515	83.0153	0.16
30	Ramnagar Stp	25.2778	83.0244	0.11

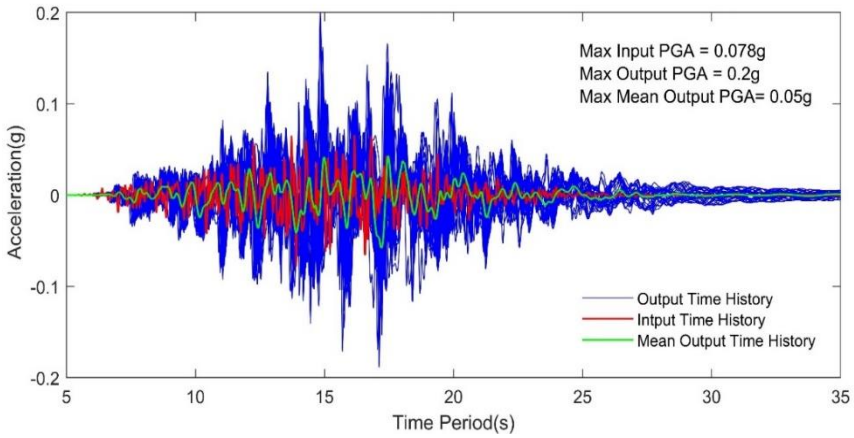

Fig. 5: Input and output time history of all sites

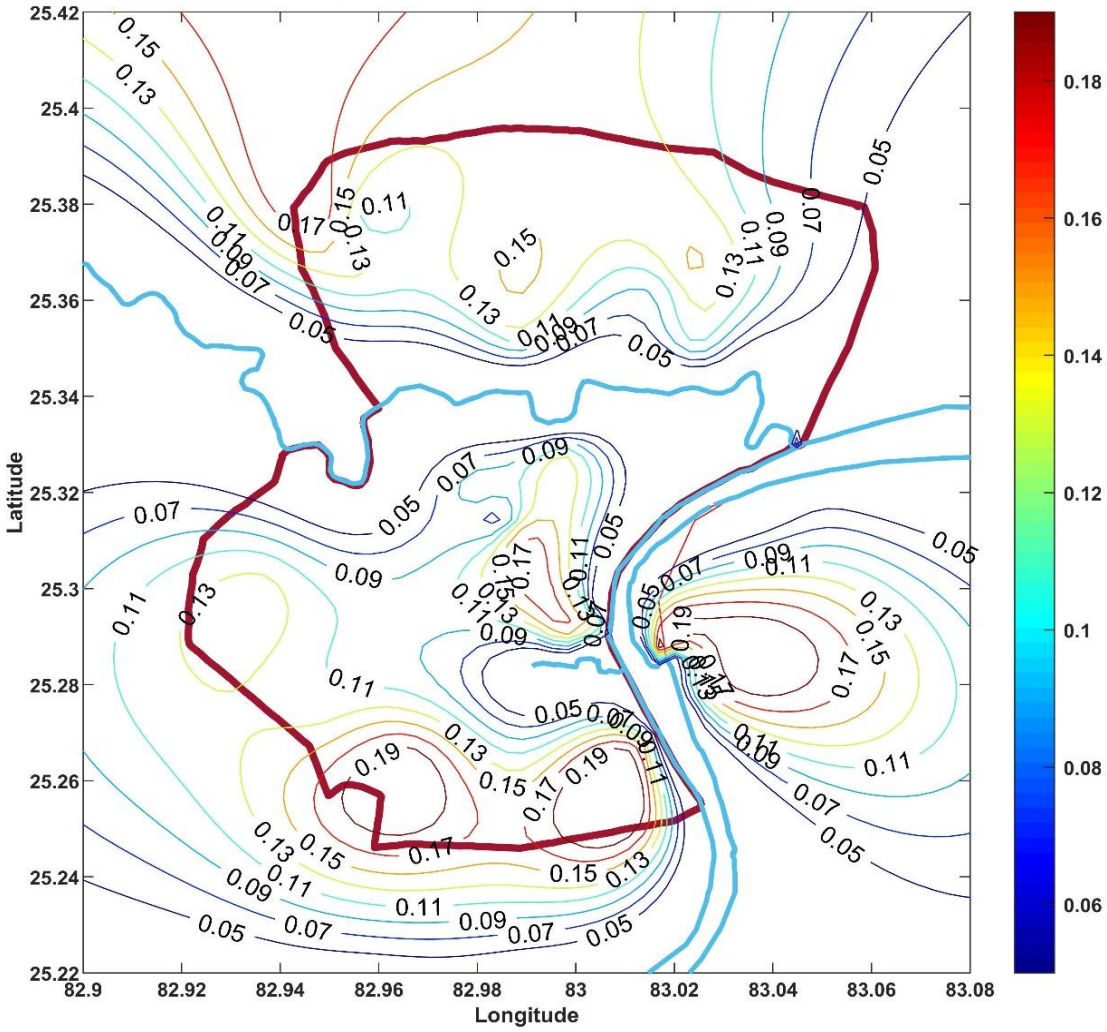

Fig. 6: Surface level output PGA

Response spectra have been made and compared with IS code 1893:2016 and are presented in fig. 7. We can conclude from the figure that for range zero-1 sec, all the sites are amplified and above the Indian seismic code (IS 1893:2016).

Highest value of spectral acceleration (0.72 g) is reported in 0.1-0.67 s duration. Further for 1–2 sec, amplification was about 2-3 times of input response spectra. For cycle 3-4 sec, very small amplification i.e. 1.0-1.3 times of input response spectra is identified. The spectral acceleration curve follows a downward trend and is below Indian seismic spectra (1893:2016) during 3.0-4.0 sec. Average response spectrum is compared with IS code 1893:2016. Amplification of average output varies between 2-5 times for entire period range.

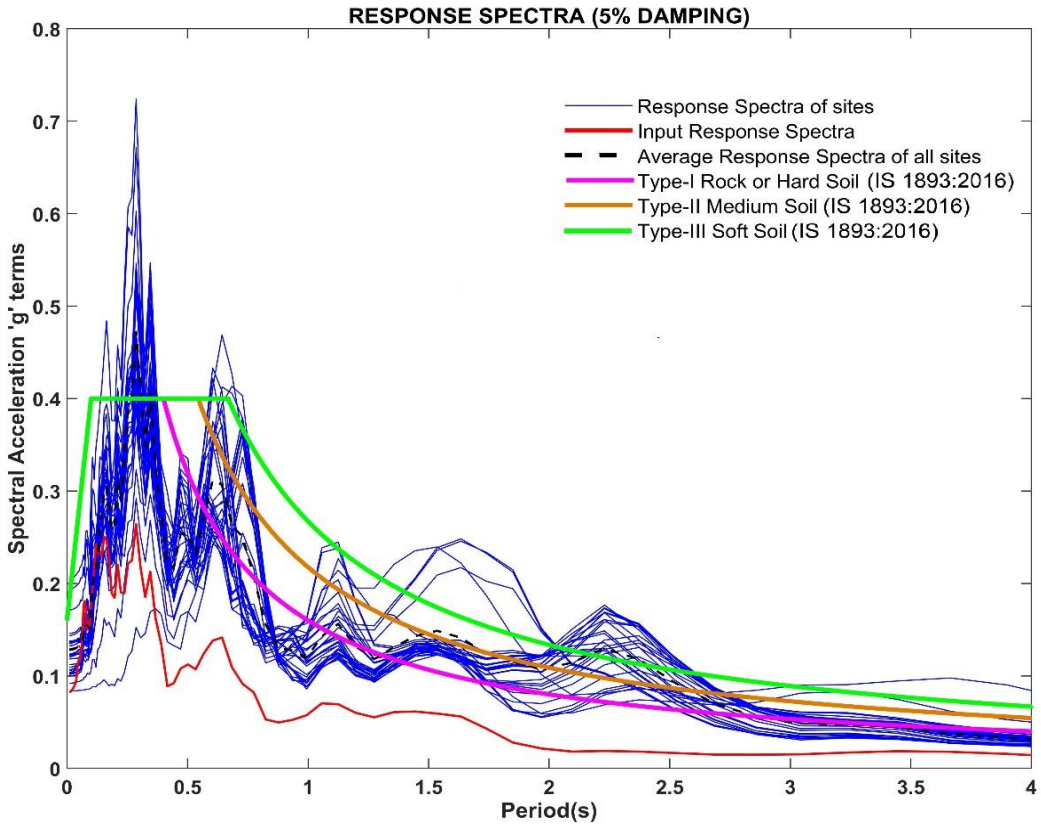

Fig. 7: Response Spectra of All Sites (5% Damping)

Peaks with a maximum spectral acceleration value are found during 0.21-0.40 s and are above the IS code curve. There is a drop in peak during 0.40 – 2.0 s and curve follows the path as of Indian Standard medium soil. Furthermore during 2.0-2.5 sec, the estimated output curve is above Indian code curve and after 2.5 sec, it follows the IS code curve.

Amplification for average response spectra with regard to input response spectra was observed 1.5, 2.5, 3.0, 6.3, 6.8 and 3.2 at time .1sec, .67sec, 1.0sec, 2.0sec, 3.0sec and 4.0sec respectively. Maximum and minimum mean spectral acceleration values are 0.47 g (at 0.28 sec) and 0.03 g (at 4.0 sec). It has been observed that developed response spectra for the city is either higher or lower when compared with Indian code. The variation is due to the incorporation of local soil effect in design of response spectra.

Conclusion

Site response analysis has been performed for Varanasi city with respect to the simulated acceleration time history for Azamgarh fault, applied as input motion at the bedrock. Geological and seismic setting for the city are briefly described. The relevant information based on subsoil conditions was gathered from geotechnical investigators for the city. Equivalent linear site response analysis was done by DeepSoil program. The results of the detailed analysis indicate that the alluvial sediments at Varanasi tend to amplify ground motion. Amplification in PGA values varies 2.5-3.0 times. While designing the structures for seismic forces, this aspect has to be taken into consideration. Further PGA contour was plotted having maximum and minimum values observed at 0.20 g at Awaleshpur and 0.06 g at Samneghat.

The maximum spectral acceleration was found to be 0.72 g at 0.67 sec. Estimated response Spectra were compared with (IS code 1893:2016) curves and it was observed that IS-1893:2016 underestimates the spectral acceleration values at most of places in Varanasi which would be a great risk from any potential earthquakes in near future. It is recommended that in addition to placing reliability on predicted PGA values, response analysis should incorporate local site effects into the evaluation of hazard parameters as effectively as possible. Moreover, this study provides assistance to structural engineers and designers for the construction of earthquake-resistant structures.

Acknowledgement

The author would like to thank the Department of Civil Engineering of Motilal Nehru National Institute of Technology Allahabad, Prayagraj U.P, India and my colleagues for providing valuable support to carry out this research.

References

1. Anbazhagan P. et al, Probabilistic seismic hazard analysis for Bangalore, *Nat. Hazards*, **48**, 145–166, https://doi.org/10.1007/s11069-008-9253-3 **(2009)**

2. Anderson J.G. and Hough S.E., A model for the shape of the fourier amplitude spectrum of acceleration at high frequencies, *Bull. Seismol. Soc. Am.*, **74**, 1969–1993 **(1984)**

3. Atkinson G.M. and Boore D.M., Earthquake Ground-Motion Prediction Equations for Eastern North America, *Bull. Seismol. Soc. Am*., **96**, 2181–2205, https://doi.org/10.1785/0120050245 **(2006)**

4. Beresnev I.A. and Atkinson G.M., Modeling finite-fault radiation from the ωn spectrum, *Bull. Seismol. Soc. Am*., **87**, 67–84 **(1997)**

5. Beresnev I.A. and Atkinson G.M., Stochastic finite-fault modeling of ground motions from the 1994 Northridge, California, earthquake. I. Validation on rock sites, *Bull. Seismol. Soc. Am*., **88**, 1392–1401 **(1998)**

6. Boore D.M. et al, Equations for estimating horizontal response spectra and peak acceleration from western North American earthquakes: A summary of re-cent work, *Seismol. Res. Lett*., **68**, 128–153 **(1997)**

7. Boore D.M., Stochastic simulation of high-frequency ground motions based on seismological models of the radiated spectra, *Bull. Seismol. Soc. Am*., **73**, 1865–1894 **(1983)**

8. Brune J.N., Tectonic stress and the spectra of seismic shear waves from earthquakes, *J. Geophys. Res*., **75**, 4997–5009, https://doi.org/10.1029/JB075i026p04997 **(1970)**

9. Chandler A.M. et al, Near-surface attenuation modelling based on rock shear-wave velocity profile, *Soil Dyn. Earthq. Eng.*, **26**, 1004–1014, https://doi.org/10.1016/j.soildyn.2006.02.010 **(2006)**

10. Choudhury D. et al, Seismic Liquefaction Hazard and Site Response for Design of Piles in Mumbai City, *Indian Geotech. J*., **45**, 62–78, https://doi.org/10.1007/s40098-014-0108-4 **(2015)**

11. Dasgupta S. et al, Seismotectonic atlas of India and its environs, Geological Survey of India, Kolkata **(2000)**

12. EPRI: Guidelines for determining design basis ground motions, United States **(1993)**

13. Gautam J.P., Ground Water Brochure of Varanasi District, U.P. CGWB, Govt. of India **(2013)**

14. Govindaraju L. and Bhattacharya S., Site-specific earthquake response study for hazard assessment in Kolkata city, India, *Nat. Hazards*, **61**, 943–965, https://doi.org/10.1007/s11069-011-9940-3 **(2012)**

15. International Code Council, International Building Code (IBC), ICC (distributed by Cengage Learning) **(2009)**

16. IS 1893: Indian Standard Criteria for Earthquake Resistant Design of Structures, Part 1 - General Provisions and Buildings, Bureau of Indian Standards, New Delhi **(2016)**

17. Jishnu R. et al, Ground response analysis of Kanpur soil along Indo-Gangetic Plains, *Soil Dyn. Earthq. Eng*., **51**, 47–57, https://doi.org/10.1016/j.soildyn.2013.04.001 **(2013)**

18. Kayal J., Microearthquake Seismology and Seismotectonics of South Asia, Springer Netherlands, Dordrecht, https://doi.org/10.1007/978-1-4020-8180-4 **(2008)**

19. Mark R.K., Application of linear statistical models of earthquake magnitude versus fault length in estimating maximum expectable earthquakes, *Geology*, **5**, 464–466 **(1977)**

20. Mitra S. et al, Crustal structure and earthquake focal depths beneath northeastern India and southern Tibet, *Geophys. J. Int.*, **160**, 227–248, https://doi.org/10.1111/j.1365-246X.2004. 02470.x **(2004)**

21. Mohanty W.K. et al, Estimation of Coda Wave Attenuation for the National Capital Region, Delhi, India Using Local Earthquakes, *Pure Appl. Geophys*, **166**, 429–449, https://doi.org/10.1007/s00024-009-0448-7 **(2009)**

22. Motazedian D. and Atkinson G., Stochastic Finite-Fault Modeling Based on a Dynamic Corner Frequency, *Bull. Seismol. Soc. Am*., **95**, 995–1010, https://doi.org/10.1785/0120030207 **(2005)**

23. Nampally S. et al, Evaluation of site effects on ground motions based on equivalent linear site response analysis and liquefaction potential in Chennai, south India, *J. Seismol*, **22**, 1075–1093, https://doi.org/10.1007/s10950-018-9751-z **(2018)**

24. Nath S.K. et al, Earthquake hazard potential of Indo-Gangetic Foredeep: its seismotectonism, hazard and damage modeling for the cities of Patna, Lucknow and Varanasi, *J. Seismol*., **23**, 725–769, https://doi.org/10.1007/s10950-019-09832-3 **(2019)**

25. NDMA, Development of Probabilistic Seismic Hazard Map of India Technical Report, Natl. Disaster Manag. Auth. **(2011)**

26. Officers of the Geological Survey of India and Roy S., The Bihar-Nepal Earthquake of 1934, *Mem. Geol. Surv. India*, **73**, 1–391 **(1939)**

27. Pallav K. et al, Surface level ground motion estimation for 1869 Cachar earthquake (M w 7.5) at Imphal city, *J. Geophys. Eng*., **7**, 321–331, https://doi.org/10.1088/1742-2132/7/3/010 **(2010)**

28. Puri N. and Jain A., Deterministic Seismic Hazard Analysis for the State of Haryana, India, *Indian Geotech. J*., **46**, 164–174, https://doi.org/10.1007/s40098-015-0167-1 **(2016)**

29. Putti S.P. et al, Estimation of ground response and local site effects for Vishakhapatnam, India, *Nat. Hazards*, **97**, 555–578, https://doi.org/10.1007/s11069-019-03658-5 **(2019)**

30. Quittmeyer R. and Jacob K., Historical and modern seismicity of Pakistan, Afghanistan, northwestern India and southeastern Iran, *Bull. Seismol. Soc. Am*., **69**, 773–823 **(1979)**

31. Raghu Kanth S.T.G. et al, Deterministic Seismic Scenarios for Imphal City, *Pure Appl. Geophys*., **166**, 641–672, https://doi.org/10.1007/s00024-009-0460-y **(2009)**

32. Raghukanth S.T.G. and Nadh Somala S., Modeling of Strong-Motion Data in Northeastern India: Q, Stress Drop and Site Amplification, *Bull. Seismol. Soc. Am*., **99**, 705–725, https://doi.org/10.1785/0120080025 **(2009)**

33. Rodolfo Saragoni G. and Hart G.C., Simulation of artificial earthquakes, *Earthq. Eng. Struct. Dyn*., **2**, 249–267, https://doi.org/10.1002/eqe.4290020305 **(1973)**

34. Satyam N.D. and Towhata I., Site-specific ground response

analysis and liquefaction assessment of Vijayawada city (India), *Nat. Hazards*, **81**, 705–724, https://doi.org/10.1007/s11069-016-2166-7 **(2016)**

35. Shukla J. and Choudhury D., Seismic hazard and site-specific ground motion for typical ports of Gujarat, *Nat. Hazards*, **60**, 541–565, https://doi.org/10.1007/s11069-011-0042-z **(2012)**

36. Shukla U.K. and Janardhana Raju N., Migration of the Ganga river and its implication on hydro-geological potential of Varanasi area, U.P., India, *J. Earth Syst. Sci*., **117**, 489–498, https://doi.org/10.1007/s12040-008-0048-4 **(2008)**

37. Singh A.P. et al, Microtremor study for evaluating the site response characteristics in the Surat City of western India, *Nat. Hazards*, **89**, 1145–1166, https://doi.org/10.1007/s11069-017-3012-2 **(2017)**

38. Singh M. et al, A Study to Establish Regression Correlation Between Shear Wave Velocity and "N"-Value for Varanasi City, India, *Proc. Natl. Acad. Sci. India Sect. A Phys. Sci*., **91**, 405–417, https://doi.org/10.1007/s40010-020-00686-w **(2021)**

39. Singh M. et al, Correlation of Shear Wave Velocity with Standard Penetration Resistance Value for Allahabad City, In Prashant A. and Sachan A., ed., Advances in Computer Methods and Geomechanics, Lecture Notes in Civil Engineering, Springer, Singapore, 467–481, https://doi.org/10.1007/978-981-15-0890-5_**(2020)**

40. Singh S.K. et al, Crustal and upper mantle structure of Peninsular India and source parameters of the 21 May 1997, Jabalpur earthquake (Mw = 5.8): Results from a new regional broadband network, *Bull. Seismol. Soc. Am*., **89**, 1631-1641 **(1999)**

41. Vucetic M. and Dobry R., Effect of Soil Plasticity on Cyclic Response, *J. Geotech. Eng*., **117**, 89–107, https://doi.org/10.1061/(ASCE)0733-9410(1991)117:1(89) **(1991)**

42. Wells D. and Coppersmith K., New empirical relationships among magnitude, rupture length, rupture width, rupture area and surface displacement, *Bull. Seismol. Soc. Am*., **84**, 974–1002 **(1994)**.

(Received 29th July 2024, revised 21st November 2024, accepted 10th December 2024)